Influence of External Stress on the Barrier Properties of Rubbers

Y. LI,[1] D. DE KEE,[1] C.F. CHAN MAN FONG,[1] P. PINTAURO,[1] A. BURCZYK[2]

[1] Department of Chemical Engineering, Tulane University, New Orleans, Louisiana 70118

[2] Defence Research Establishment Suffield, Box 4000, Medicine Hat, Alberta T1K 8K6, Canada

Received 23 November 1998; accepted 25 January 1999

ABSTRACT: The effect of an external stress on the barrier properties of natural, bromobutyl, and nitrile rubber were studied using a modified ASTM permeation method. Stress-induced changes such as a decrease in the breakthrough time with mechanical elongation was observed. Upon application of a small mechanical deformation, little change was observed in terms of steady-state permeation flux. On the other hand, a stress-enhanced diffusion was observed for most of the solvent/rubber pairs studied.
 J Appl Polym Sci 74: 1584–1595, 1999

Key words: diffusion; membranes; rubber; deformation; stress

INTRODUCTION

Polymeric membranes are used in various environments, where they are subjected to interactions with aggressive liquids, thermal degradation, crazing, mechanical deformation, swelling, etc. The barrier properties of polymers may be described by parameters such as breakthrough time, permeability, diffusion coefficient, and solubility and they are also affected by forces such as mechanical stresses. The stress experienced by a polymer membrane may be a combination of an applied external stress as well as a stress associated with sample swelling as a result of polymer–solvent contact. The effects of deformation on the transport properties have been studied by various authors, and no definite conclusions can as yet be drawn due to the complexity of the processes involved.

It was found that the permeability P and the average diffusion coefficient D for various gases through PVC,[1] poly(vinylidene fluoride),[2] polypropylene,[3] polystyrene,[4] polyethylene,[4–6] and Gutta–Percha (*trans*-polyisoprene)[7] decreases with the drawing ratio due to increase in the crystallinity and to structural changes caused by uniaxial or biaxial elongation. Sometimes, an increase, followed by a decrease in the values of P and D, has been observed as the drawing ratio increases. This is the case for the permeation of gases in a stretched emulsion acrylic multipolymer,[8] in poly(ethylene terephthalate) film,[9] in uniaxially drawn polycarbonate film,[10,11] in biaxially oriented polystyrene,[12] and in polyethylene and polypropylene.[13] Such a stress-enhanced transport is attributed to an increase of free volume caused by tensile stress.[9,10,11,13] The permeability of N_2 and He in lightly vulcanized natural rubber was observed to be constant when a sample was stretched biaxially up to 24% strain.[13] The permeability of H_2 through vulcanized natural rubber was also studied by Fauchon et al.[14] They found that P initially increases with increasing elongation, attains a maximum, and subsequently decreases with increasing elongation. This cycle repeats itself, and they related the permeability to the Young's modulus.

Correspondence to: D. De Kee.

Journal of Applied Polymer Science, Vol. 74, 1584–1595 (1999)
 CCC 0021-8995/99/061584-12

Table I Some Properties of Rubber Materials

	NR	BIIR	(NBR)
Structure	*cis*-1,4-Polyisoprene	Brominated (Isobutylene + isoprene)	Acrylonitrile + butadiene
Density at 298 K ($\times 10^{-3}$ kg m^{-3})	1.140	1.094	1.203
Glass transition temperature T_g (K)	211.5	207.2	263
Elongation at rupture (%)	578	991	621
Ultimate tensile strength (N m^{-2})	0.174	0.138	0.179
Solubility parameter δ (MPa)$^{1/2}$	16.6		20.2

Liquid transport through polymeric materials is frequently related to polymer swelling and crazing. The effect of stress on the transport of liquids in polymers is more complex. A decrease in P and D caused by mechanical drawing was observed for the transport of CH_2Cl_2 (DCM) in drawn polyethylene,[15] for various organic vapors in polyethyene,[16,17] for DCM in LDPE,[18,19] for toluene in highly oriented polypropylene,[20] for orange-II in nylon 66,[21] and for dye in polyamide fibers.[22] Such a decrease is usually attributed to a decrease in the free volume and an increase in the crystallinity and to a structural change from a spherulitic film to a less-permeable fiber structure.[15] Takagi et al.[23] reported a slight initial increase followed by a decrease in the diffusion coefficient of dye in drawn polyamide fibers. Barrie and Platt[24,25] reported no measurable changes in the solubility and permeability of hydrocarbons through stretched rubber at lower elongations up to the point where crystallization occurs. Highly stretched, unvulcanized rubber had a lower permeability than that of unstretched rubber due to the crystallization caused by drawing.[26] A diffusion coefficient component of methanol in uniaxially drawn poly(ether sulfone)[27] of hexane in polystyrene[28] and of camphorquinone in uniaxially drawn polycarbonate films[29] was found to increase with increasing draw ratio in the direction perpendicular to the polymer stretching. More recently, strain-enhanced transport was also measured for toluene and water through poly(aryl ether ether ketone) (PEEK).[30,31] The effect of mechanical stress on the transport properties of several liquids through PVC and HDPE geomembranes was recently studied by Xiao et al.[32] They found that a uniaxial tensile stress leads to a slight increase in the diffusion coefficients of liquid penetrants through PVC.

We note that the permeation measurement in the above studies was mostly performed after external mechanical stress release,[1–10,15–23,26–29] that is, only the effect caused by the residual stress was observed. Few studies dealt with the transport of organic liquids through stretched rubber films. The aim of this work was to study the influence of an external mechanical stress on the permeation properties of various solvents through deformed rubber polymers.

EXPERIMENTAL

Materials

Three polymeric materials, natural rubber (NR), that is, SMR-L; NBR (NBR), that is, Krynac 40E65 at 39.8% ACN; and bromobutyl rubber (BIIR), that is, Polysar Bromobutyl X2, were studied and some of their physical properties are given in Table I. The samples were molded from milled blanks prepared from laboratory-mixed rubber compounds. The solvents used were dichloromethane (DCM), acetone, benzene, and toluene. They were of laboratory or analytical grade and their properties are listed in Table II.

Tensile Test

The mechanical properties of the rubber samples were studied using an Instron tensile testing machine (Model TTD with a 200-lb tension load cell). The small tensile load cell allows for the application of a small force on the sample, and different scales (5, 10, 50, 100, and 200 lb) can be selected. The tensile test was performed at 298 K according to the ASTM D412 standard tensile test method designed for rubber properties in tension. A grip separation speed of 50 cm min^{-1} was selected. The full scale of 50 lb was used.

The tensile stress (σ) and strain (ε) are calculated from

Table II Physical Properties of the Solvents Used[34]

	Acetone	Benzene	DCM	Toluene
Formula	CH_3COCH_3	C_6H_6	CH_2Cl_2	$C_6H_5CH_3$
MW	58.08	78.11	84.94	92.14
Density at 298 K ($\times 10^{-3}$ kg m^{-3})	0.7899	0.87865	1.319	0.8669
Molar volume at 298 K ($\times 10^{6}$ m^3 mol^{-1})	74.0	89.4	63.9	106.8
Boiling point (K)	329.2	353.1	312.4	383.6
δ (MPa)$^{1/2}$	20.3	18.8	19.8	18.2

$$\sigma = f/A_0 \quad (1)$$

$$\varepsilon = 100(L - L_0)/L_0 \quad (2)$$

where f is the load at specified elongation; A_0, the cross-sectional area of the unstrained specimen; and L_0 and L, the initial and the final lengths between the reference marks, respectively.

Permeation Measurements Under External Stress

A modified ASTM permeation cell (ASTM F-739-85), combined with a home-made stainless-steel drawing apparatus, were used to perform the measurements. The cell consists of two chambers separated by the elongated polymer membrane. The sample is drawn along one direction and kept under stress while permeation tests are performed. Equally spaced reference lines were drawn on the sample. The sample was fixed at one end by a clamp and was then stretched in one direction with a draw stem along a draw track. The displacement of the lines allow for the computation of the elongation in the test section. The top and bottom parts were firmly clamped with the elongated sample in between. The whole setup was placed in a temperature-controlled chamber. A permeation test was initiated by introducing a penetrant into the upstream chamber. This top part of the ASTM cell was closed to prevent vaporization of chemicals. This is now time $t = 0$ for the experiment. The volume of the challenge chamber used to hold the solvent is about 70 mL, and the volume of the medium collecting chamber is about 90 mL. The apparatus used for the permeation tests was described in detail elsewhere.[32,33] The sample thickness was determined using a micrometer to within 10^{-5} m. The rubber sample (0.15×0.15 m^2) was stretched uniaxially at a crosshead speed of 4 cm min^{-1} until the desired elongation is achieved. The carrier gas flowing through the collecting chamber was nitrogen at a flow rate of 50 mL min^{-1}. The solvent permeating through the membrane was automatically sampled by a Valco programmed valve and analyzed by a GC flame-ionization detection system (Hewlett–Packard, Model 5790 A series chromatograph). The permeation measurement started immediately after the solvent was charged into the challenge chamber. The amount of solvent permeating through the membrane is proportional to the peak area recorded by the GC, which was calibrated with a diffusion cell using the same carrier gas flow rate at the same temperature. The mass balance was checked with a gravity cell. Permeation measurements were performed under an open-loop mode. The temperature of the chamber was 298 $\pm$ 0.5 K.

RESULTS

Stress–Strain Curves

When a mechanical elongation (ε) is applied to a polymeric material, the stress (σ) increases with the deformation, and this is associated with changes in the internal energy (E) and entropy (S).[35] The stress exerted on the polymeric material may result in crystallization (or chain orientation) and crazing, which leads to a change in its permeation properties. The deformation caused by mechanical elongation may be recoverable or may be irreversible, depending on the applied stress.

Elastomers (natural and synthetic rubbers) are amorphous polymers to which various ingredients are added. Rubber is unique in being soft, highly extensible, and highly elastic. The typical high elasticity of rubber arises from its linear molecu-

lar structure. Figure 1 illustrates the stress–strain curves measured at 298 K for the three rubber materials used. At small strains, rubber behaves as a linear elastic substance and the range of linear elasticity depends on the material. The stress–strain curves for NR and NBR are similar and their elastic moduli are of the same order of magnitude, but that for BIIR is markedly different with a much lower elastic modulus. At low values of ε, σ is a slowly increasing function of ε. When ε exceeds 200%, the stress increases more rapidly with increasing elongation. These phenomena are explained via Gaussian chain statistics and network theory.[35] NRand NBR rupture at lower values of ε compared to that of BIIR (Table I). Following rupture, all three rubber samples can recover about 80–85% of their original dimensions. Some mechanical properties of the three rubbers are given in Table I.

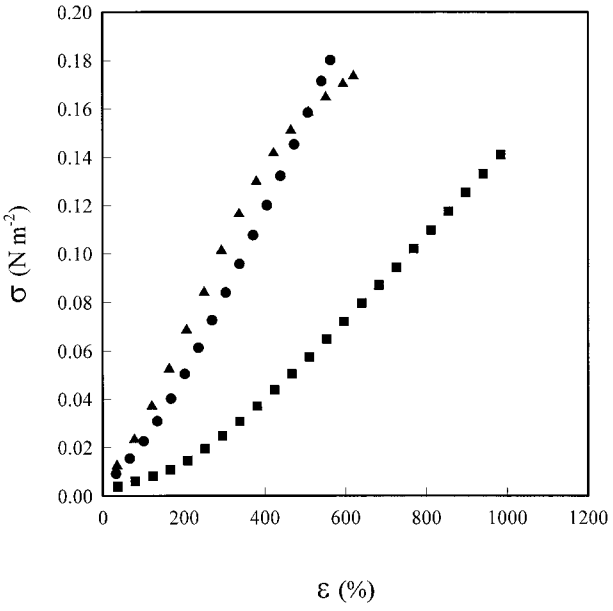

Figure 1 Stress–strain curves measured at 298 K for (●) NR; (■) BIIR; (▲) NBR.

Permeation Under External Stress

The permeation properties of polymers depend strongly on the polymer structure as well as on the nature of the solvent. Figures 2 and 3 show the permeation flux F against time t for DCM and acetone through various rubbers. Figures 4 and 5 illustrate the $F - t$ curves for various solvents permeating through different rubbers at 20% elongation. The effect of elongation on the $F - t$ curves is shown in Figures 6 and 7 for the case of

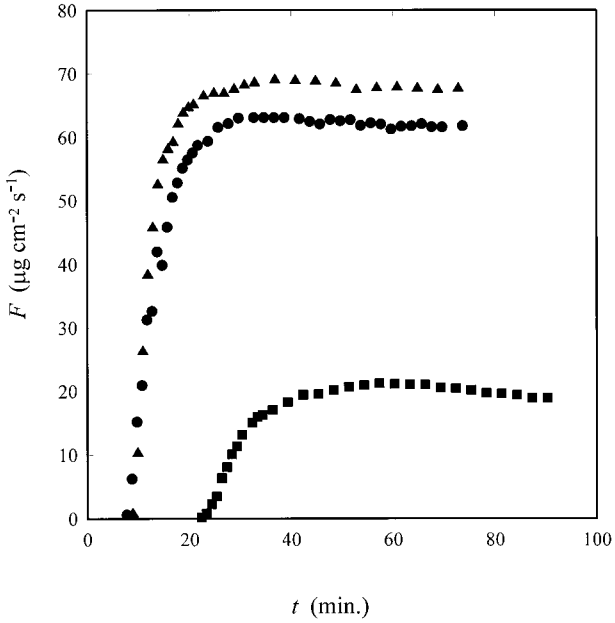

Figure 2 Permeation flux F against time t for DCM through different rubbers at 298 K: (●) NR; (■) BIIR; (▲) NBR.

acetone through NR and for the case of DCM through BIIR, respectively. For most solvent/rubber pairs, F is a monotonically increasing function of t until the steady state is reached. For DCM through BIIR, the flux time curve has a maximum, probably associated with the reorientation or redistribution of crystallites.[25] A similar feature was observed in the permeation of various solvents through PVC and HDPE geomembranes.[32,33,36] The values of the breakthrough time t_b and the steady-state flux F_s, which are two important parameters determining the barrier properties of polymers, are given in Tables III–V for different solvent/rubber pairs. The experimental errors for t_b and F_s for most solvent/rubber systems are 3 and 5%, respectively. For acetone/BIIR, the errors are about 5% for t_b and 10% for F_s.

Diffusion Coefficients

It is possible to estimate the diffusion coefficients from $F - t$ curves. Three methods are widely used. For small values of t, it has been shown that[32,33,37]

$$\ln(Ft^{1/2}) = \ln\left[2C\left(\frac{D_0}{\pi}\right)^{1/2}\right] - \frac{L^2}{4D_0t} \qquad (3)$$

where L is the thickness of the membrane; C, the concentration at the polymer–penetrant inter-

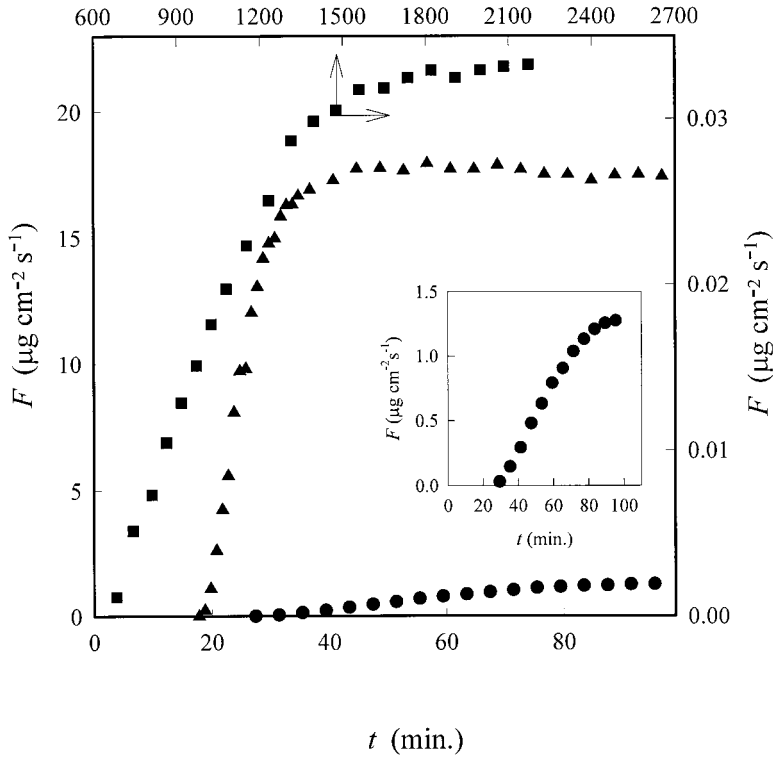

Figure 3 Permeation flux F against time t for acetone through different rubbers at 298 K: (●) NR; (■) BIIR; (▲) NBR.

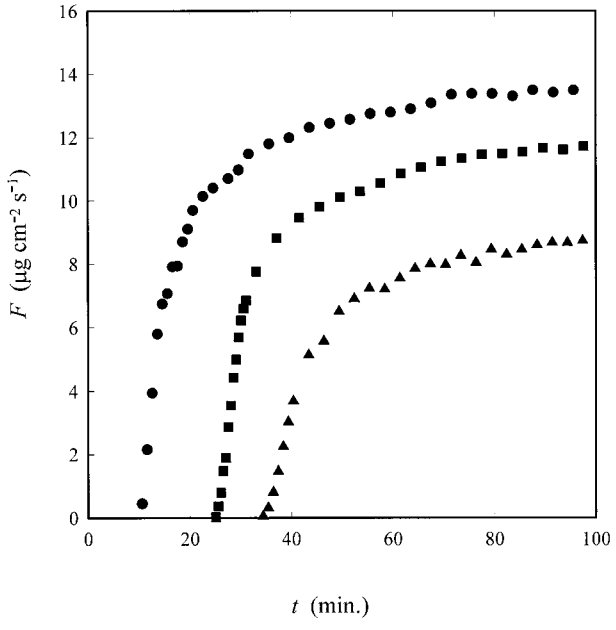

Figure 4 Permeation flux F against time t for toluene through different rubbers at 20% elongation at 298 K: (●) NR; (■) BIIR; (▲) NBR.

face; and D_0, the limiting diffusion coefficient at zero penetrant concentration. Although the concentration of the penetrant in the challenge chamber is high, its concentration at the interface is initially approximately zero. A plot of $\ln(Ft^{1/2})$ against t^{-1} yields a straight line; the coefficient D_0 is determined from the slope. The linear region is confined to a short time interval immediately following the breakthrough time.

The relationship between F and t can also be given by[37]

$$\ln\left(1 - \frac{F}{F_s}\right) = \ln 2 + \ln \sum_{n=1}^{\infty} \left[(-1)^{n+1} \exp\left(-\frac{n^2\pi^2 D}{L^2} t \right) \right] \quad (4)$$

For $t \gg 1$, eq. (4) can be approximated as

$$\ln\left(1 - \frac{F}{F_s}\right) = \ln 2 - \frac{\pi^2 D}{L^2} t \quad (5)$$

A plot of $\ln(1 - F/F_s)$ against t yields a straight line which allows for an easy determination of D.

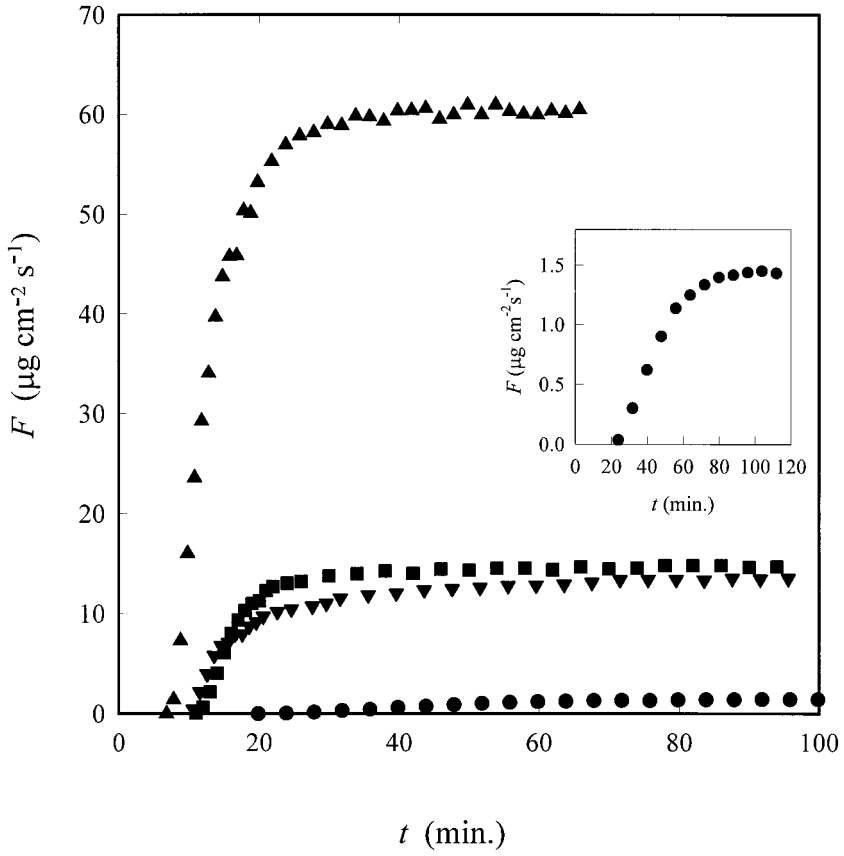

Figure 5 Permeation flux F against time t for solvents through NR at 20% elongation at 298 K: (●) acetone; (■) benzene; (▲) DCM; (▼) toluene.

In this case, the plot is observed to be a straight line in the region where $0.5 \leq F/F_s \leq 0.98$. This diffusion coefficient can be considered to be the diffusion coefficient when the system is near its equilibrium and is denoted by D_e.

Another diffusion coefficient which can be deduced from eq. (5) is the average diffusion coefficient $D_{1/2}$.[33,39,40] If the time at which $F/F_s = 0.5$ is denoted by $t_{1/2}$, then it follows from eq. (5) that

$$D_{1/2} = \frac{2L^2 \ln 2}{\pi^2 t_{1/2}} = \frac{L^2}{7.119 t_{1/2}} \qquad (6)$$

We estimate that the errors involved in calculating D_0, $D_{1/2}$, and D_e are 12, 4, and 7%, respectively. The values of D_0, $D_{1/2}$, and D_e for the various systems are given in Tables VI–VIII.

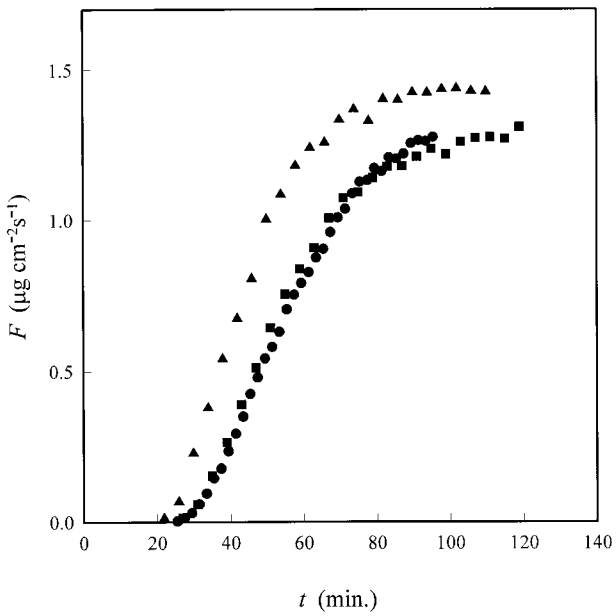

Figure 6 Effect of elongation on the permeation flux F for acetone through NR at 298 K. Elongation (%): (●) 0; (■) 10; (▲) 20.

DISCUSSION

From the data obtained, it can be seen that the values of F_s and t_b depend on the combination of

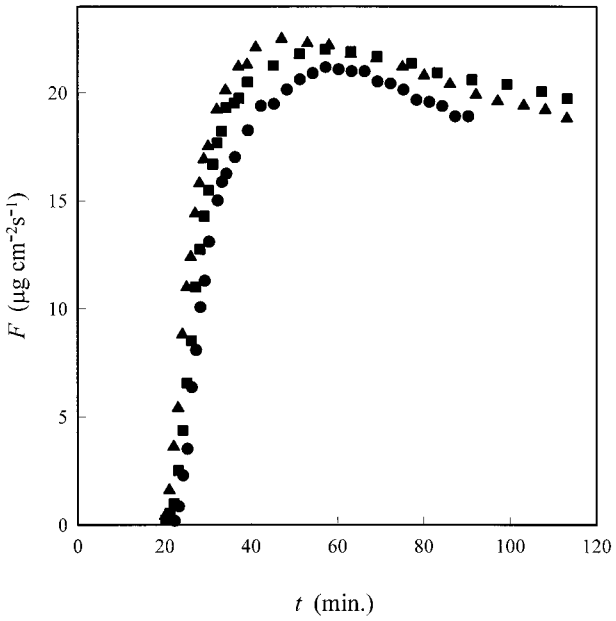

Figure 7 Effect of elongation on the permeation flux F for DCM through BIIR at 298 K. Elongation (%): (●) 0; (■) 10; (▲) 20.

the penetrant and rubber. For the same rubber, the penetrant that has the lowest value of t_b has the highest value of F_s. For all three rubbers considered in the present study, DCM has the lowest t_b and the highest F_s. In the diffusion through NR and BIIR, acetone has the highest t_b and the lowest F_s compared to the other solvents. However, for NBR, it is toluene that has the lowest F_s and the highest t_b among the three solvents.

The permeation properties are often related to the molecular size of the penetrant molecules. For molecules of similar shape and chemical nature, the permeation rate is found to decrease with increasing molecular dimension. This is consistent with our experimental results for benzene and toluene; a slightly higher value of F_s is observed for benzene. Other contributing factors are the degree of swelling and polarity.

It was reported[41] that the equilibrium swelling for NR in acetone is 12–22%, and in benzene (or toluene), it is 200–600%, depending on the additives. The higher permeation flux may be associated with the higher degree of swelling and this is consistent with the observation that F_s for the acetone/NR pair is much lower than that for benzene/NR. We also note that the permeation flux of acetone through NBR becomes much higher than that of toluene, because polar solvents like acetone induce a high degree of swelling in polar rubbers such as NBR.[41] Nitrile–butadiene rubber is a random copolymer of acrylonitrile (mass fraction of 0.4) and butadiene, in which strong polarity is attributed to the acrylonitrile. Polar compounds tend to permeate through polar membranes faster than through nonpolar compounds.[42]

Another parameter which may be associated with the flux F_s is the so-called solubility parameter δ, which is defined as the square root of the cohesive energy density and describes the attractive strength between molecules of the materials.[34] Actually, δ can also be related to the polarity. It was shown[43] that the closer the values of δ for the rubber–solvent pair the higher the F_s.

Table III Breakthrough Time, t_b (min) and Steady-State Permeation Flux F_s (μg cm^{-2} s^{-1}) for Different Solvents Permeating Through NR at 298 K

		Elongation (%)				
Solvents		0	5	10	15	20
Acetone	t_b (min)	26.4	25.3	25.0	22.5	20.8
(0.75 mm)[a]	F_s	1.28	1.31	1.31	1.40	1.44
Benzene	t_b (min)	12.2	12.1	11.9	11.5	11.0
(0.78 mm)[a]	F_s	15.1	14.9	14.8	14.8	14.7
DCM	t_b (min)	7.9	7.5	7.3	6.5	6.3
(0.77 mm)[a]	F_s	61.5	59.2	58.1	59.4	59.6
Toluene	t_b (min)	13.2	12.5	11.7	11.1	11.0
(0.77 mm)[a]	F_s	12.5	13.5	14.4	13.9	13.5

[a] The numbers in the brackets are the original thicknesses of the rubber sheet.

Table IV Breakthrough Time, t_b (min) and Steady-State Permeation Flux F_s (μg cm^{-2} s^{-1}) for Different Solvents Permeating Through BIIR at 298 K

		Elongation (%)				
Solvents		0	5	10	15	20
Acetone	t_b (min)	680	575	550	540	535
(0.82 mm)[a]	F_s	0.033	0.075	0.097	0.108	0.040
DCM	t_b (min)	22.3	21.3	20.7	20.6	19.6
(0.85 mm)[a]	F_s	21.2	21.6	22.0	22.4	22.5
Toluene	t_b (min)	30.9	28.1	26.0	26.0	25.1
(0.81 mm)[a]	F_s	11.0	11.2	11.3	11.3	11.7

[a] The numbers in the brackets are the original thicknesses of the rubber sheet.

Table II gives the values of δ for various solvents. The values of δ for NR and for NBR containing 30% acrylonitrile are 16.6 and 20.2 $(MPa)^{1/2}$, respectively. For BIIR, δ is not available; however, the solubility parameter for the copolymers of isobutylene and isoprene is 15.9 $(MPa)^{1/2}$. We note that the bromobutyl samples used were 1.5 wt % isoprene prior to the bromination reaction. We can assume that the solubility parameter of the bromobutyl product should be almost identical to that of the isobutylene–isoprene copolymer. It is seen that the rule stated earlier is valid for toluene and acetone but not for DCM. The difference in δ between acetone and NR or BIIR is larger than that for benzene or toluene; therefore, acetone has a lower permeation rate in NR and BIIR than those of benzene and toluene (Tables III and IV). The difference in δ between acetone and NBR is smaller than that of toluene; correspondingly, its permeation rate is larger than that for toluene. The exception is DCM: Its permeation rate is always the highest among the systems studied. This can be attributed to the possibility of a chemical reaction occurring between DCM and the membranes and that δ is not the sole factor controlling the permeation process. The dark brown color of the solvent observed after permeation suggests that the additives in the rubbers might have dissolved in the DCM.

We now consider the effect of extension during the permeation tests. For all the systems studied, the breakthrough time t_b decreased with increasing extension. This may, in part, be associated with the thinning effect caused by the elongation. The thicker the sample, the larger the t_b and the lower the F_s. The influence of the elongation on the steady-state flux F_s again depends on the solvent and rubber combination. Three cases were observed:

(a) F_s is a nondecreasing function of the elongation;

Table V Breakthrough Time, t_b (min) and Steady-State Permeation Flux F_s (μg cm^{-2} s^{-1}) for Different Solvents Permeating Through NBR at 298 K

		Elongation (%)				
Solvents		0	5	10	15	20
Acetone	t_b (min)	18.8	17.8	16.8	16.4	16.2
(0.81 mm)[a]	F_s	17.5	17.4	17.4	17.3	17.4
DCM	t_b (min)	8.8	8.6	8.6	8.2	7.8
(0.81 mm)[a]	F_s	68.1	68.8	68.8	70.0	70.4
Toluene	t_b (min)	42.5	40.5	39.9	37.2	34.9
(0.78 mm)[a]	F_s	8.2	8.4	8.4	8.6	8.7

[a] The numbers in the brackets is the original thickness of the rubber sheet.

Table VI Effect of Elongation on Diffusion Coefficients D_0, $D_{1/2}$, and D_e for Various Solvents Permeating Through NR at 298 K

Solvents	Diffusion Coefficient ($\times 10^8$ cm^2 s^{-1})	Elongation (%) 0	5	10	15	20
Acetone	D_0	5.8	6.7	7.2	7.7	8.9
	$D_{1/2}$	24.2	25.0	25.5	28.3	30.6
	D_e	25.7	28.6	29.1	32.9	36.0
Benzene	D_0	12.9	12.3	11.6	10.7	15.2
	$D_{1/2}$	85.0	84.8	85.9	86.7	84.5
	D_e	210.0	191	163.0	142.0	103.0
DCM	D_0	23.7	25.9	27.2	36.8	39.3
	$D_{1/2}$	110.6	116.4	119.6	125.0	116
	D_e	193.4	205.6	210.3	205.4	211.2
Toluene	D_0	13.1	13.8	14.7	11.5	11.2
	$D_{1/2}$	70.3	71.9	80.7	86.8	90.9
	D_e	73.6	75.0	81.2	89.0	104.6

(b) F_s initially decreases and then increases with elongation; and

(c) F_s initially increases and then decreases with elongation.

Systems that belong to category (a) are acetone through NR and NBR, DCM through BIIR and NBR, and toluene through BIIR and NBR. Benzene/NR and DCM/NR are in category (b) and acetone/BIIR and toluene/NR are in category (c). It can be expected that benzene and toluene would have more or less similar permeation properties due to their similar chemical structure and this is confirmed in Figure 5. The values of t_b, F_s, and D_0 for benzene and toluene through NR are indeed comparable (see Tables III and VI). However, the effect of an external stress on F_s puts them into different categories and this should be further explored.

Figures 6 and 7 show typical $F - t$ curves for acetone/NR and DCM/BIIR pairs obtained at various elongations. It can be seen that the curves are similar, suggesting the possibility of a master curve. Figures 8 and 9 show examples of such master curves for toluene/NBR and DCM/NBR where we have plotted F/F_s against $(t - t_b)F_s$. Similar, master curves were observed for all systems studied.

Table VII Effect of Elongation on Diffusion Coefficients D_0, $D_{1/2}$, and D_e for Various Solvents Permeating Through BIIR at 298 K

Solvents	Diffusion Coefficient ($\times 10^8$ cm^2 s^{-1})	Elongation (%) 0	5	10	15	20
Acetone	D_0	0.66	0.55	0.60	0.65	0.65
	$D_{1/2}$	1.6	1.8	1.8	1.9	1.9
	D_e	4.9	4.8	5.1	4.7	4.6
DCM	D_0	7.4	8.8	9.2	9.9	10.2
	$D_{1/2}$	59.8	60.3	61.5	64.8	68.6
	D_e	178.0	195.0	204.0	219.0	220.0
Toluene	D_0	4.1	6.7	7.5	7.7	8.2
	$D_{1/2}$	41.5	47.1	48.1	48.0	49.2
	D_e	42.9	49.7	51.6	52.5	55.3

Table VIII Effect of Elongation on Diffusion Coefficients D_0, $D_{1/2}$, and D_e for Various Solvents Permeating Through NIR at 298 K

Solvents	Diffusion Coefficient ($\times 10^8$ cm^2 s^{-1})	Elongation (%) 0	5	10	15	20
Acetone	D_0	8.9	10.4	10.5	11.9	15.6
	$D_{1/2}$	65.1	67.1	67.6	72.0	72.3
	D_e	224	236	237	249	246
DCM	D_0	46.0	52.0	56.0	63.4	73.0
	$D_{1/2}$	132.0	136.0	137.0	146.0	145.0
	D_e	233.0	239.0	240.0	266.0	296.0
Toluene	D_0	2.3	2.7	3.2	3.7	3.8
	$D_{1/2}$	27.3	28.5	28.9	30.5	34.0
	D_e	68.5	68.6	75.8	78.2	80.2

The diffusion coefficients D_0, $D_{1/2}$, and D_e are related to F_s and t_b. For a particular rubber, the solvent that is associated with the highest value of D_e (or D_0, $D_{1/2}$) has the highest value of F_s and the lowest value of t_b. Tables VI–VIII and Figure 10 show that in all cases $D_e > D_{1/2} \gg D_0$. If the diffusion is Fickian, $D_0 = D_{1/2} = D_e$. In the present case, the diffusion is non-Fickian. Several authors[44,45] proposed that the diffusion coefficient D is an increasing function of the concentration C, and D can then be given by[45]

$$D = D_0 \exp(\gamma C) \tag{7}$$

where γ is a constant which is a measure of the plasticizing action of the liquid on the polymer membrane. When γ is relatively small, eq. (7) can be approximated by

$$D = D_0(1 + \gamma C) \tag{8}$$

The coefficients D_0 and D can be associated with the diffusion coefficients as C tends to zero and to

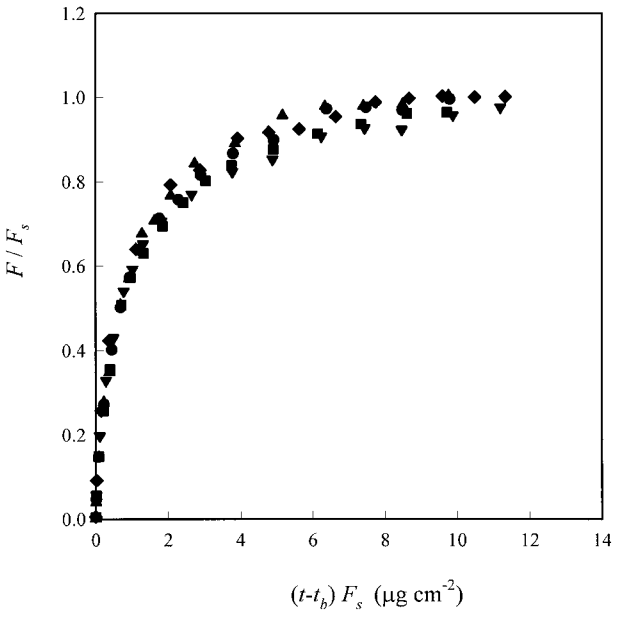

Figure 8 Plot of F/F_s against $(t - t_b)F_s$ for toluene through NBR at 298 K. Elongation (%): (●) 0; (■) 5; (▲) 10; (▼) 15; (♦) 20.

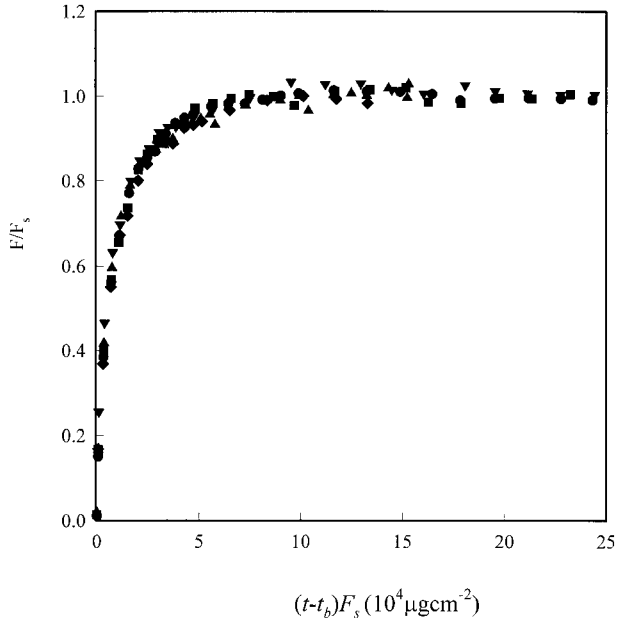

Figure 9 Plot of F/F_s against $(t - t_b)F_s$ for DCM through NBR at 298 K. Elongation (%): (●) 0; (■) 5; (▲) 10; (▼) 15; (♦) 20.

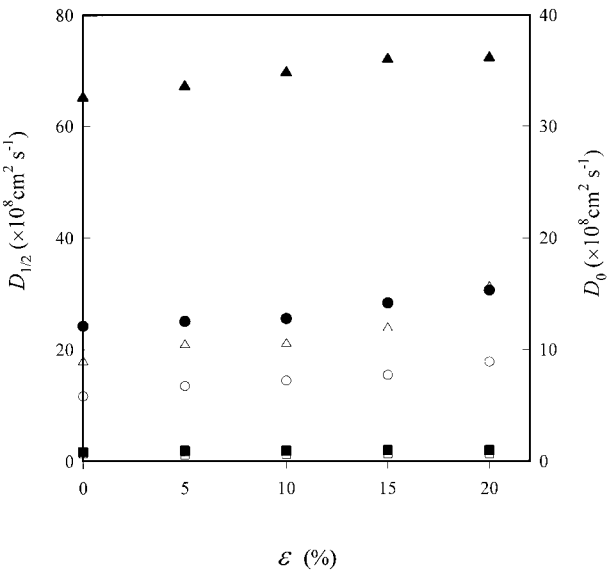

Figure 10 Effect of elongation on (closed symbols) the average diffusion coefficient $D_{1/2}$ and (open symbols) the limiting diffusion coefficient D_0 for acetone through the three rubbers at 298 K: (●,○) NR; (■,□) BIIR; (▲,△) NBR.

its equilibrium value, respectively. Similarly, $D_{1/2}$ can be interpreted as the diffusion coefficient associated with $F = 0.5F_s$. Since D is assumed to be an increasing function of C, it follows that $D_e > D_{1/2} > D_0$. The coefficients D_0, $D_{1/2}$, and D_e provide a range for the diffusion coefficient, associated with the fact that the diffusion of a solvent in a polymer may produce a nonhomogeneous spatial concentration distribution with time.[46–48] Therefore, it is expected that the diffusion coefficients obtained by different methods may correspond to different stages of the process.

The effects of the applied elongation on D_0, $D_{1/2}$, and D_e are given in Tables VI–VIII. For most solvent/rubber systems, increasing elongation results in an increase in D_0, $D_{1/2}$, and D_e. For benzene/NR and toluene/NR, D_0 initially decreases and then increases with elongation. For the acetone/BIIR system, the coefficients D_0, $D_{1/2}$, and D_e are not affected by the applied stress.

The stress-induced change may be attributed to changes in the size of the nanometer-scale voids, which can be considered to be part of the "free volume" of the polymer structure. The free-volume theory is widely used to interpret changes in the diffusion coefficient D caused by extension.[49,50] According to this theory, D can be written as[49]

$$D = D_1 \exp\left(-\frac{A_D}{f}\right) \quad (9)$$

where D_1 and A_D are assumed to be independent of the applied extension. f is the free-volume fraction and it increases linearly with tensile uniaxial elastic straining.[49] In this case, D increases with increasing elongation.

It was assumed in eq. (9) that the change in free volume caused by mechanical stretching is the main factor determining D. However, as mentioned earlier, the transport process depends on several factors. Many changes are associated with the permeation of a solvent through a polymer under an external stress. For example, stress-induced crystallization[1–7, 26,49] and solvent-induced crystallization[51,52] are often observed, leading to a decrease in the permeability and diffusion coefficient. Daldsen[26] found that highly stretched, unvulcanized rubber had a lower water permeability than that of unstretched rubber because this process crystallizes the rubber. On the other hand, a microporouslike structure may be induced by a solvent-drawing process, as observed by Williams.[53]

The changes in the permeation properties of the membrane due to an applied extension may also be attributed to the change in the thickness of the membrane during measurement.[54] Since the real thickness after stretching and during testing is difficult to obtain, all our computations are based on the original thickness before extension. On the one hand, sample thickening results from polymer swelling and the thickness change due to swelling is time-dependent. On the other hand, sample thinning is caused by the applied elongation. We observed that the thickening effect and thinning effect are approximately equal at small elongation.

An extension of the classical Fickian diffusion by considering a concentration-dependent diffusion coefficient cannot adequately describe a general diffusion process. More realistic models that include a stress and a relaxation process have been considered and need further study.[55,56]

CONCLUSIONS

The barrier properties of NR, BIIR, and NBR under an applied uniaxial stress were studied by a modified ASTM permeation method. Breakthrough time, steady-state flux, and diffusion coefficients (D_0, $D_{1/2}$, and D_e) were determined. It was found that the breakthrough time decreases with increasing elongation. Upon the application of a small mechanical deformation, little change was observed in terms of the steady-state flux,

which may or may not increase with elongation, depending on the solvent–rubber combination. Master curves were found to adequately represent flux–time profiles for all systems studied. Stress-enhanced diffusion was observed for most solvent–rubber systems.

One of the authors (P.P.) acknowledges support by the U.S. Department of Defense through the Tulane/Xavier Center for Bioenvironmental Research.

REFERENCES

1. El-Hibri, M. J.; Paul, D. R. J Appl Polym Sci 1985, 30, 3649.
2. El-Hibri, M. J.; Paul, D. R. J Appl Polym Sci 1986, 31, 2533.
3. Taraiya, A. K.; Orchard, G. A. J.; Ward, I. M. J Appl Polym Sci 1990, 41, 1659.
4. Wang, L. H.; Porter, R. S. J Polym Sci 1984, 22, 1645.
5. Holden, P.S.; Orchard, G. A. J.; Ward, I. M. J Polym Sci Polym Phys Ed 1985, 23, 2295.
6. Webb, J. A.; Bower, D. I.; Ward, I. M.; Cardew, P. T. J Polym Sci Part B Polym Phys 1993, 31, 743.
7. Arvanitoyannis, I.; Heath, R. Polym Int 1992, 29, 165.
8. El-Hiibri, M. J.; Paul, D. R. J Appl Polym Sci 1986, 31, 2583.
9. Vieth, W. R.; Matulevicius, E. S.; Mitchell, S. R. Koll Z 1967, 220, 49.
10. Smith, T. L.; Adam, R. E. Polymer 1981, 22, 299.
11. Dickinson, J. T.; Jensen, L. C.; Langford, S. C.; Dion, R. P. J Polym Sci Part B Polym Phys 1993, 32, 993.
12. Rosen, B. J. Polym Sci 1960, 47, 19.
13. Yasuda, H.; Stanett, V.; Frish, H. L.; Perterlin, A. Makromol Chem 1964, 73, 188.
14. Fauchon, A. J.; Lenoir, J.; Escoubes, M.; Quinson, J. F.; Lallemand, A.; Eyraud, P.; Eyraud, C. Rev Gen Caout Plast 1970, 47, 861.
15. Williams, J. L.; Peterlin, A. J Polym Sci A-2 1971, 9, 1483.
16. Peterlin, A. Williams, J. L. Stannett, V. J. Polym Sci A-2, 1967, 5, 957.
17. Marshall, J. M.; Hope, P. S.; Ward, I. M. Polymer 1982, 23, 142.
18. Araimo, L.; De Candia, F.; Vittoria, V. J Polym Sci Polym Phys Ed 1978, 16, 2087.
19. De Candia, F.; Russo, R.; Vittoria, V. J Polym Sci Polym Phys Ed 1982, 20, 269.
20. Choy, C. L.; Leung, W. P.; Ma, T. L. J Polym Sci Polym Phys Ed 1984, 22, 707.
21. Davis, G. T.; Taylor, H. S. Text Res J 1965, 35, 405.
22. Takagi, Y. J Appl Polym Sci 1965, 9, 3887.
23. Takagi, Y.; Hattori, H. J Appl Polym Sci 1965, 9, 2167.
24. Barrie, J. A.; Platt, B. J Polym Sci 1961, 49, 479.
25. Barrie, J. A.; Platt, B. J Polym Sci 1961, 54, 261.
26. Daldsen, J. W. V. Rubb Chem Technol 1943, 16, 388.
27. Chau, C. C.; Fear, D. L.; Wessling, R. A. Polymer 1989, 30, 2087.
28. Nicolais, L.; Drioli, E.; Hopfenberg, H. B.; Apicella, A. Polymer 1979, 20, 459.
29. Xia, J. L.; Wang, C. H. J Polym Sci Part B Polym Phys 1992, 30, 1437.
30. Wolf, C. J.; Fu, H. J Polym Sci Part B Polym Phys 1996, 34, 75.
31. Wolf, C. J.; Fu, H. J Polym Sci Part B Polym Phys 1995, 33, 331.
32. Xiao, S.; Moresoli, C.; Bovenkamp, J.; De Kee, D. J Appl Polym Sci 1997, 65, 1833.
33. Xiao, S.; Moresoli, C.; Bovenkamp, J.; De Kee, D. J Appl Polym Sci 1997, 63, 1189.
34. Brandrup, J.; Immergut, E. H. Polymer Handbook, 3rd ed.; Wiley-Interscience: New York, 1989.
35. Treloar, L. R. G. The Physics of Rubber Elasticity; Oxford University: Oxford, 1958.
36. Nelson, G. O.; Lum, B. Y.; Carlson, G. J.; Wong, C. M.; Johson, J. S. Am Ind Hyg Assoc J 1981, 42, 217.
37. Rogers, W. A.; Buritz, R. S.; Alpert, D. J Appl Phys 1954, 25, 868.
38. Ziegel, K. D.; Frensdorff, H. K.; Blair, D. E. J Polym Sci Part A-2 Polym Phys 1969, 7, 809.
39. Vahdat, N. J Appl Polym Sci 1991, 42, 3165.
40. Suzuki, F.; Onozato, K. J Appl Polym Sci 1982, 27, 4229.
41. Aminabhavi, T. M.; Harogoppad, S. B.; Khinnavar, R. S.; Balundgi, R. H. JMS-Rev Macromol Chem Phys C 1991, 31, 433.
42. Sweeny, R. F.; Rose, A. Ind Eng Chem Prod Res Dev 1965, 4, 248.
43. Huang, R. Y. M.; Lin, V. J. C. J Appl Polym Sci 1968, 12, 2615.
44. Neogi, P. J Polym Sci Part B Polym Phys 1993, 31, 699.
45. Li, N. N.; Long, R. B. In Progress in Separation Purification; Perry, E. S.; Vanoss, C. J., Eds.; Wiley: New York, 1970; p 153.
46. Harogoppad, S. B.; Aminabhavi, T. M. Polymer 1991, 32, 870.
47. Ramsey, D. R. Geosynthetics 93, Vancouver, Canada, 1993; p 645.
48. Rogers, C. E.; Machin, D. Crit Rev Macromol Sci 1960, 1, 245.
49. Peterlin, A. J Macromol Sci-Phys B 1975, 11, 57.
50. Xia, J. L.; Wang, C. H. J Polym Sci Part B Polym Phys 1992, 30, 1437.
51. Arzak, A.; Eguiazabal, J. I.; Nazabal, J. J Polym Sci Part B Polym Phys 1994, 32, 325.
52. Cornelis, H.; Kander, R. G. Polymer 1996, 37, 5627.
53. Williams, J. Am Chem Soc Div Org Coat Plast Chem Pap 1974, 34, 475.
54. Alfrey, T.; Gurance, E. F.; Lloyd, W. G. J Polym Sci Part C 1966, 12, 249.
55. Edwards, D. A.; Cohen, D. S. AIChE J 1995, 41, 2345
56. Chan Man Fong, C. F.; Moresoli, C.; Xiao, S.; Li, Y.; Bovenkamp, J.; De Kee, D. J Appl Polym Sci 1998, 67, 1885.